From Racemic Mixtures of Chiral π-Donor Molecules to Mixed Stacks of H-Bonded Centrosymmetrical Dimers of Cation and Anion Radicals with Singlet–Triplet Excitations: The Example of $[(\pm)Me_3TTF-C^*H(MeOH)^{\bullet+}]_2[TCNQ^{\bullet-}]_2$ (TTF = Tetrathiafulvalene; TCNQ = Tetracyanoquinodimethane)

Anne Dolbecq, Marc Fourmigué, and Patrick Batail*

Laboratoire de Physique des Solides, Unité Associée au CNRS No 2, Université de Paris-Sud, 91405 Orsay, France

Claude Coulon

Centre de Recherche Paul Pascal du CNRS, 33600 Pessac, France

Received March 8, 1994. Revised Manuscript Received June 2, 1994®

Lithiation of Me_3TTF, and subsequent reaction with ClCOMe followed by reduction with $NaBH_4$ afford the racemic alcohol $(\pm)Me_3TTF-C^*H(Me)OH$. Single crystals of the title compound $[(\pm)Me_3TTF-C^*H(Me)OH^{\bullet+}]_2[TCNQ^{\bullet-}]_2$ were obtained, and their structure was determined by X-ray diffraction, revealing an unusual type of mixed stacking where the chiral π-donor and the acceptor molecule are associated within a ···DDAA··· sequence. The room temperature ESR spectrum is characteristic of two different triplet Frenkel exciton systems. From the analysis of the single-crystal ESR measurements the singlet–triplet activation energy and the fine structure tensor orientation were determined for both triplet excitations. The relationship between these parameters and the structure allowed us to propose an interpretation of the nature of both excitations. The role of the hydrogen bonding between the dimers of donors and acceptors is discussed.

Introduction

Following the identification of single layers of orthogonal dimers within the so-called κ-phase arrangement in a series of organic conductors and superconductors based on bisethylenedithiotetrathiafulvalene and a few of its unsymmetrical derivatives,[1] there is a strong current research effort devoted to the design of similar constructions based on dimers of cation radical molecules.[2,3]

The purpose of this paper is to provide a first example where a *racemic* mixture of π-donor molecules is engaged in the synthesis of charge-transfer or cation radical salts in order to enforce the formation of *dimers* in the solid state, unless, of course, spontaneous enantiomeric separation occurs to yield optically active charge transfer salts, a much unpredictable, albeit certainly rather appealing, alternative.

We therefore report the synthesis of the racemic π-donor title molecule which, because of its hydroxyl-substituted chiral center, presents the additional capability to be engaged in hydrogen-bonded networks in the solid state, an important structural functionality expected to favor significant orientation effects of the coupled dimeric conjugated π-systems.

In that respect, it should be noted that while significant contributions have focused for some time now on the creation of hydrogen-bond patterns of intermolecular associations in the organic solid state,[4] their role in the design and control of the electronic properties of conducting or magnetic molecular solids, by either imposing specific architectures (indirect electronic effect),[2,5–9] or upon direct proton–electron coupling phenomena,[10,11] remains largely unexplored.

An illustration of how this set of unprecedented molecular features may operate is provided by the unique

® Abstract published in *Advance ACS Abstracts*, August 15, 1994.

(1) (a) Williams, J. M.; Ferraro, J. R.; Thorn, R. J.; Carlson, K. D.; Geiser, U.; Wang, H. H.; Kini, A. M.; Whangbo, M.-H. In *Organic Superconductors*; Prentice Hall: Englewood Cliffs, NJ, 1992, p 65. (b) Yamoshi, H.; Komatsu, T.; Matsukawa, N.; Saito, G.; Mori, T.; Kusunoki, M.; Sakaguchi, K. *J. Am. Chem. Soc.* **1993**, *115*, 11319.

(2) Blanchard, P.; Boubekeur, K.; Sallé, M.; Duguay, G.; Jubault, M.; Gorgues, A.; Martin, J. D.; Canadell, E.; Auban-Senzier, P.; Jérome, D.; Batail, P. *Adv. Mater.* **1992**, *4*, 579.

(3) Batsanov, A. S.; Bryce, M. R.; Cooke, G.; Heaton, J. N.; Howard, J. A. K. *J. Chem. Soc., Chem. Commun.* **1993**, 1701.

(4) Etter, M. C. *Acc. Chem. Res.* **1990**, *23*, 120.

(5) (a) Whangbo, M.-H.; Jung, D.; Ren, J.; Evain, M.; Novoa, J. J.; Mota, F.; Alvarez, S.; Williams, J. M.; Beno, M. A.; Kini, A. M.; Wang, H. H.; Ferraro, J. R. In *The Physics and Chemistry of Organic Superconductors*; Saito, G., Kagoshima, S., Eds.; Springer-Verlag: Berlin, 1990; p 262. (b) Novoa, J. J.; Mota, F.; Whangbo, M.-H.; Williams, J. M. *Inorg. Chem.* **1991**, *30*, 54. (c) Novoa, J. J.; Whangbo, M.-H.; Williams, J. M. *Chem. Phys. Lett.* **1991**, *180*, 241.

(6) Susuki, T.; Yamochi, H.; Srdanov, G.; Hinkelmann, K.; Wudl, F. *J. Am. Chem. Soc.* **1989**, *111*, 3108.

(7) Davidson, A.; Boubekeur, K.; Pénicaud, A.; Auban, P.; Lenoir, C.; Batail, P.; Hervé, G. *J. Chem. Soc., Chem. Commun.* **1989**, 1373.

(8) Pénicaud, A.; Boubekeur, K.; Batail, P.; Canadell, E.; Auban-Senzier, P.; Jérome, D. *J. Am. Chem. Soc.* **1993**, *115*, 4101.

(9) Hernandez, E.; Mas, M.; Molins, E.; Rovira, C.; Veciana, J. *Angew. Chem., Int. Ed. Engl.* **1993**, *32*, 884.

(10) (a) Torrance, J. B.; Girlando, A.; Mayerle, J. J.; Crowley, J. I.; Lee, V. Y.; Batail, P.; La Placa, J. J. *Phys. Rev. Lett.* **1981**, *47*, 1747. (b) Batail, P.; La Placa, S. J.; Mayerle, J. J.; Torrance, J. B. *J. Am.Chem. Soc.* **1981**, 103, 951.

(11) Inabe, T.; Okaniwa, K.; Okamoto, H.; Mitani, T.; Maruyama, Y.; Tadeka, S. *Mol. Cryst. Liq. Cryst.* **1992**, *216*, 229.

0897-4756/94/2806-1413$04.50/0

stuctural pattern and magnetic properties achieved for the title charge-transfer complex.

Experimental Section

Synthesis of 4,3′,4′-Trimethyltetrathiafulvalene (4). The phosphonate ester **2** was prepared according to a previously described procedure,[12] starting from the dithiolium salt **1** (25.82 g, 0.1 mol) and $P(OMe)_3$ (12.80 g, 0.1 mol). The compound **2** was further reacted with *t*-BuOK (11.22 g, 0.1 mol) and then the imminium salt **3** in dry THF at −7 8°C. After warming up to −20 °C, Et_2O was added to precipitate the remaining salts; the filtered solution was concentrated, diluted with toluene and treated with AcOH. The solution was washed with water, dried over $MgSO_4$, concentrated and chromatographed (silica gel, toluene) to afford **4** as orange needles, after recrystallization from MeCN; yield 11.9 g (48%); mp 103–104 °C. ^1H NMR ($CDCl_3$/TMS) δ = 1.93 (s, 6H, CH_3), δ = 2.13 (s, 3H, CH3), δ = 5.82 (s, 1H).

Synthesis of 3-Acetyl-4,3′,4′-trimethyltetrathiafulvalene (6) and 1,1-Bis(4,3′,4′-trimethyltetrathiafulvalen-3-yl)-ethanol (7). To a solution of **4** (1 g, 4.06 mmol) in dry Et_2O (100 mL) at −78 °C under nitrogen was added $NH(i\text{-}Pr)_2$ (0.64 mL, 4.46 mmol) followed by BuLi (2.5M, in hexane, 1.8 mL, 4.46 mmol). The suspension was stirred for 1 h and added dropwise to a solution of freshly distilled ClCOMe (1.16 mL, 16.24 mmol) in Et_2O at −78 °C. The yellow mixture turned red immediately. The solution was slowly warmed up to room temperature. The solvent was evaporated, 100 mL of toluene and 100 mL of water were added to the residue, and the organic layer was dried over $MgSO_4$ and concentrated. Flash chromatography (silica gel, toluene) afforded first unreacted **4** (300 mg, 30%), followed by the alcohol **7** (307 mg, 14%) and the ketone **6** (130 mg, 11%). A sample was recrystallized from acetone affording **6** as dark red needles; mp 116–117 °C. Anal. Calcd for $C_{11}H_{12}OS_4$ (Found): C, 45.80 (46.00); H, 4.19 (4.49); S, 44.46 (44.92). ^1H NMR ($CDCl_3$/TMS): δ = 1.93 (s, 6H, CH_3), δ = 2.30 (s, 3H, CH_3), δ = 2.37 (s, 3H, CH_3). The alcohol **7** (307 mg) was recrystallized from toluene affording brown crystals of the toluene solvate (150 mg); mp 211–212 °C. Calcd for $C_{20}H_{22}OS_8{\cdot}0.5C_7H_8$ (Found): C, 48.57 (49.81); H, 4.51 (4.55); S, 44.15 (43.71). ^1H NMR ($CDCl_3$/TMS) δ = 1.67 (br s, 3H, CH_3), δ = 1.93 (br s, 18H, CH_3).

Synthesis of 1-(4,3′,4′-Trimethyltetrathiafulvalen-3-yl)-ethanol (8). To a solution of **3** (290 mg, 1 mmol) in 100 mL of EtOH was added $NaBH_4$ (95 mg, 2.5 mmol). The mixture was refluxed for 30 min; at that time complete decoloration was observed. The solvent was evaporated, 50 mL of cyclohexane and 50 mL of water were added, the organic layer was dried over $MgSO_4$, and the cyclohexane was evaporated. Recrystallization from cyclohexane/THF (4:1) afforded **8** as orange crystals; yield 170 mg (58%); mp 116–117 °C. Anal. Calcd for $C_{11}H_{14}OS_4$ (Found): C, 45.49 (45.66); H, 4.86 (4.62); O, 5.51 (5.57); S, 44.15 (44.02). ^1H NMR ($CDCl_3$/TMS): δ = 1.40 (d, 3H, J = 6 Hz, CH_3), δ = 1.93 (br s, 9H, CH_3), δ = 4.83 (q, 1H, 6Hz).

Synthesis of 8–TCNQ. The solvents were dried over activated alumina before use. To a solution of **8** (5 mg, 0,02 mmol) in 5 mL of MeCN was added slowly a solution of TCNQ (4 mg, 0.02 mmol). The mixture turned green immediatly. The solvent was slowly evaporated at room temperature affording black shiny bulky crystals after two days. Anal. Calcd for $C_{23}H_{18}N_4OS_4$ (Found): C, 55.85 (55.93); H, 3.67 (3.81); N, 11.33 (11.23); O, 5.51 (5.57); S, 25.92 (26.15).

Crystallography. The crystallographic data are summarized in Table 1. A black crystal of approximate dimensions 0.09 × 0.12 × 0.45 mm^3 was used for data collection on an Enraf-Nonius CAD-4F diffractometer. The data were collected using the $\omega/2\theta$ scan. The number of total reflections measured were 4990 ($1 \leq \theta \leq 26°$; $\pm h$, $\pm k$, $+l$) giving 4605 independent reflections. The structure was solved using direct methods. The non-hydrogen atoms were refined anisotropically by full-matrix least-squares methods. Hydrogen atoms were included in structure factor calculations at ideal positions and not refined. The final cycle of least-squares refinement was based on 2688 reflections [$I \geq 3\sigma(I)$] and 289 variable parameters. The maximum and minimum peaks on the final difference Fourier map correspond to 0.86 and −0.88 e $Å^{-3}$. All computer programs are from Xtal 3.2.[13] The final positional parameters are given in Table 2. The atom labeling for the donor and acceptor molecules are given in Figure 1.

ESR Measurements. ESR spectra were recorded on a Varian X-band spectrometer operating at 9.3 GHz and equipped with a Oxford ESR 900 helium cryostat.

Table 1. Crystallographic Data for 8–TCNQ

chem formula	$C_{46}H_{36}S_8O_2N_8$
f_w	989.46
cryst system	triclinic
space group (No.)	$P\bar{1}$ (No. 2)
a, Å	9.285(2)
b, Å	10.911(2)
c, Å	12.952(1)
α, deg	67.64(1)
β, deg	75.26(1)
γ, deg	95.57(1)
V, $Å^3$	1145.7(4)
Z	2
d_{calcd}, g cm^{-3}	1.434
λ, Å	0.71069
μ, cm^{-1}	4.28
T, K	293
$R(F_o)^a$	0.055
$R_w(F_o)^a$	0.054

^{a} $R = \sum(|F_o| - |F_c|)/\sum|F_o|$ and $w = 1$.

Table 2. Atomic Coordinates and Equivalent Isotropic Thermal Parameters for 8–TCNQ

atom	x	y	z	U_{eq},^{a} $Å^2$
		8		
S(1)	0.6167(2)	0.8661(2)	0.3690(2)	0.0553(9)
S(2)	0.3963(2)	1.0672(2)	0.3144(2)	0.059(1)
S(3)	0.4088(2)	0.7288(2)	0.6248(2)	0.0581(9)
S(4)	0.1892(2)	0.9290(2)	0.5727(2)	0.061(1)
C(1)	0.4484(8)	0.9284(8)	0.4146(7)	0.053(4)
C(2)	0.3574(8)	0.8692(8)	0.5255(7)	0.052(4)
C(3)	0.6458(9)	0.9777(8)	0.2256(7)	0.057(4)
C(4)	0.5453(9)	1.0684(8)	0.2010(7)	0.059(4)
C(5)	0.2455(9)	0.7113(8)	0.7321(7)	0.061(4)
C(6)	0.1450(9)	0.8043(8)	0.7076(7)	0.061(4)
C(7)	0.784(1)	0.9546(8)	0.1474(8)	0.073(4)
C(8)	0.542(1)	1.172(1)	0.0845(8)	0.082(5)
C(9)	0.233(1)	0.591(1)	0.8413(8)	0.080(5)
C(10)	−0.006(1)	0.809(1)	0.7842(9)	0.086(5)
C(11)	0.8878(8)	0.8982(8)	0.2097(7)	0.055(3)
O	0.746(1)	0.871(1)	0.0861(9)	0.196(8)
H	0.7027	0.7605	0.1667	0.035
		TCNQ		
C(12)	−0.0318(8)	0.5379(7)	0.6576(6)	0.049(3)
C(13)	−0.0627(8)	0.6529(8)	0.5686(6)	0.054(3)
C(14)	0.0364(9)	0.7040(8)	0.4658(6)	0.054(3)
C(15)	0.1761(8)	0.6462(7)	0.4424(6)	0.049(3)
C(16)	0.2100(9)	0.5327(8)	0.5328(7)	0.058(4)
C(17)	0.1082(9)	0.4811(8)	0.6355(7)	0.056(4)
C(18)	−0.1376(9)	0.4833(7)	0.7654(6)	0.054(3)
C(19)	−0.273(1)	0.5439(9)	0.7911(7)	0.061(4)
C(20)	−0.1041(9)	0.3708(9)	0.8551(8)	0.063(4)
C(21)	0.2815(8)	0.6977(7)	0.3343(6)	0.053(3)
C(22)	0.2553(9)	0.8131(9)	0.2452(7)	0.063(4)
C(23)	0.421(1)	0.6393(8)	0.3134(7)	0.061(4)
N(1)	−0.3812(9)	0.5961(9)	0.8124(7)	0.092(5)
N(2)	−0.0751(9)	0.2794(9)	0.9276(7)	0.090(4)
N(3)	0.2295(9)	0.90987(8)	0.1743(7)	0.089(4)
N(4)	0.5344(8)	0.5903(8)	0.2993(7)	0.080(4)

^{a} $U_{eq} = {}^1/_3\sum_i\sum_j U_{ij}a_i^*a_j\bar{a}_i\bar{a}_j$.

(12) (a) Lerstrup, K. A.; Johannsen, I.; Jørgensen, M. *Synth. Met.* **1988**, *27*, B9. (b) Jørgensen, M.; Lerstrup, K. A.; Bechgaard, K. *J. Org. Chem.* **1976**, *41*, 2855. (c) Fourmigué, M.; Krebs, F. C.; Larsen, J. *Synthesis* **1993**, *5*, 509.

(13) Hall, S. R.; Flack, H. D.; Stewart, J. M. **1992**, Editors *Xtal3.2 Reference Manual*, Universities of Western Australia, Australia, Geneva, Switzerland, and Maryland.

Scheme 1

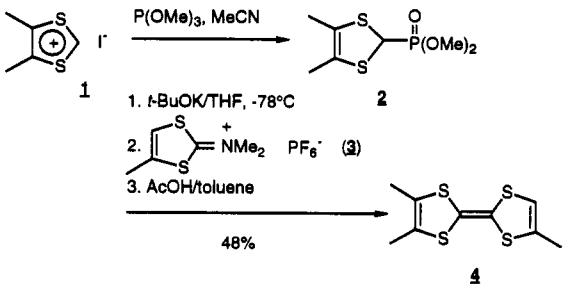

Scheme 2

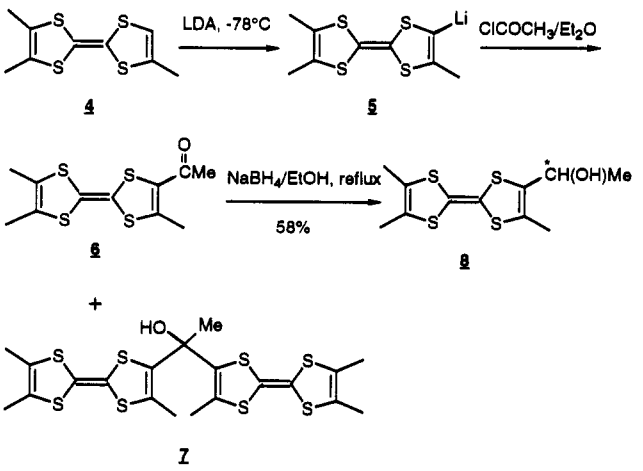

Results and Discussion

Synthesis. Several tetrathiafulvalenes bearing a primary alcohol functionality have been recently reported. While Green[14] described the reaction of the tetrathiafulvalenyllithium derivative with formaldehyde to afford the unstable 3-hydroxymethyltetrathiafulvalene, Gorgues et al. investigated the reduction of the easily prepared ester derivatives of TTF and EDT–TTF with $NaBH_4$ or $LiAlH_4$ to yield mono-,[15] bis-,[15] and tetra[16] -substituted hydroxymethyl TTFs. Other primary alcohols were also reported with larger alkyl[17] or aryl[18] spacers between tetrathiafulvalenyl and hydroxyl moieties.

To improve the stability of the alcohol derivatives of tetrathiafulvalene, we chose to start from an alkyl-substituted TTF,[19] such as Me_3TTF (4). The compound 4 was synthesized as described in Scheme 1.[12] The secondary alcohol derivative of 4 was prepared from the prochiral ketone 6, readily prepared from the trimethyltetrathiafulvalene 4 (Scheme 2) by lithiation[14,19,20] and reaction with acetyl chloride.[21] In addition to the ketone 6, some amount of tertiary alcohol 7 was obtained, the latter was obtained by the reaction of the trimethyltetrathiafulvalenyllithium on the ketone 6. Reduction of 6 with $NaBH_4$ afforded the secondary alcohol 8 as a racemic mixture in 58% yield (Scheme 2).

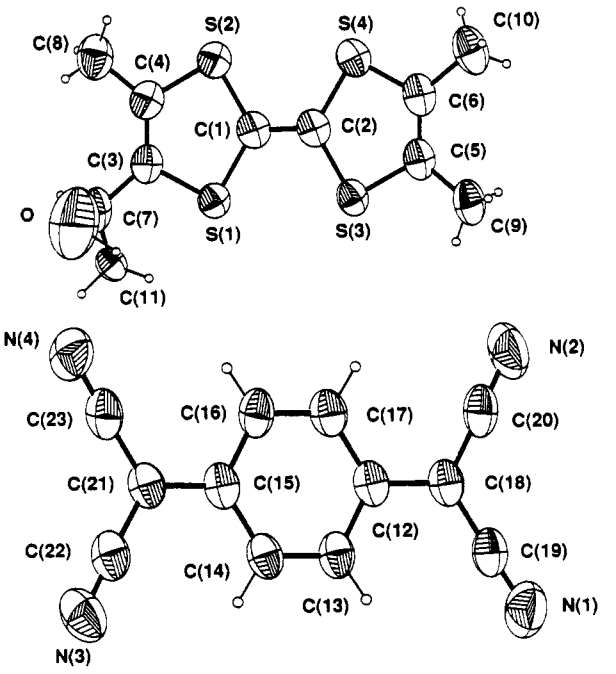

Figure 1. Molecular structures and atom labeling for 8–TCNQ.

In cyclic voltammetry experiments, 8 exhibits two reversible oxidation waves at +0.25 and +0.62 V/vs SCE, essentially identical to those of Me_4TTF (+0.24 and +0.62 V/vs SCE).[22] Single crystals of the 1:1 salt 8–TCNQ were obtained by slow evaporation of an equimolar acetonitrile solution of the two compounds.

Structure of 8–TCNQ. Two independent molecules, (±)Me_3TTF–C*H(Me)OH (8) and TCNQ, are identified in the asymmetric unit of the triclinic unit cell of the compound. Their molecular structures are depicted in Figure 1 and selected bond distances are given in Table 3. As exemplified in Figure 2, centrosymmetrical dimers of donor and acceptor molecules are associated within mixed stacks in a ···DDA··· sequence which differ from the ···DADA··· pattern common to most TTF-based mixed-stack complexes.[23] This pattern is also unusual for TCNQ complexes of other electron donor molecules since only three examples have been reported, namely, (3,3′-diethyloxacyanine)(TCNQ),[24] (NBP)(TCNQ)[25] (NBP: *N*-butylphenazidium), and (1-ethyl-2,3-dimethylimidazolium)-(TCNQ).[26] The molecular planes are normal to the

(14) Green, D. C. *J. Org. Chem.* **1979**, *44*, 1477.
(15) Blanchard, Ph.; Sallé, M.; Duguay, G.; Jubault, M.; Gorgues, A. *Tetrahedron Lett.* **1992**, *33*, 2685.
(16) Sallé, M.; Gorgues, A.; Jubault, M.; Boubekeur, K.; Batail, P. *Tetrahedron* **1992**, 48, 3081.
(17) (a) Moore, A. J.; Bryce, M. R. *J. Chem. Soc., Chem. Commun.* **1991**, 1638. (b) Marshallsay, G. J.; Bryce, M. R.; Cooke, G.; Jørgensen, T., Becher, J.; Reynolds, C. D.; Wood, S. *Tetrahedron* **1993**, *49*, 6849. (c) Moore, A. J.; Bryce, M. R.; Cooke, G.; Marshallsay, G. J.; Skabara, P. J.; Batsanov, A. S., Howard, J. A. K.; Daley, S. T. A. K. *J. Chem. Soc., Perkin Trans. 1* **1993**, 1403.
(18) Pittman, Cu. Jr.; Narita, M.; Liang, Y. F. *J. Org. Chem.* **1976**, *41*, 2855.
(19) Me_3TTF derivatives have been shown to exhibit better crystallinity and lower chemical reactivity than the unsubstituted TTF analogues: Fourmigué, M.; Huang, Y. S. *Organometallics* **1993**, *12*, 797. This is mainly due to the steric and electron-donating effect of the methyl substituents (or other substituents like $S(CH_2)_2S$ in BEDT–TTF) and is not primarily related to the oxidation potential of the molecule. For example, the monoalcohol derivative $TTF–CH_2OH$[14] is much more unstable than the tetrasubstituted $TTF(CH_2OH)_4$,[16] albeit the latter oxidizes at a lower potential.
(20) Jarshow, S.; Fourmigué, M.; Batail, P. *Acta. Crystallogr. C* **1993**, *49*, 1936.
(21) Cooke, G.; Bryce, M. R.; Petty, M. C.; Ando, D. J.; Hurthouse, M. B. *Synthesis* **1993**, 465.
(22) Schukat, G.; Richter, A. M.; Fanghanel, E. *Sulfur Rep.* **1987**, *7*, 155.
(23) Mori, T.; Wu, P.; Imaeda, K.; Enoki, T.; Inokuchi, H.; Saito, G. *Synth. Met.* **1987**, *19*, 545.
(24) Grossel, M. C.; Evans, F.; Hriljac, J. A., Prout, K.; Weston, S. C., *J. Chem. Soc., Chem. Commun.* **1990**, 1494.
(25) (a) Harms, R. H.; Keller, H. J.; Nöthe, D.; Wehe, D.; Heimer, N.; Metzger, R. M.; Gundel, D.; Sixl, H. *Mol. Cryst Liq. Cryst.* **1982**, *85*, 249. (b) Metzger, R. M.; Heimer, N. E.; Gundel, D.; Sixl, H.; Harms, R. H.; Keller, H. J.; Nöthe, D.; Wehe, D. *J. Chem. Phys.* **1982**, *77*, 6203.

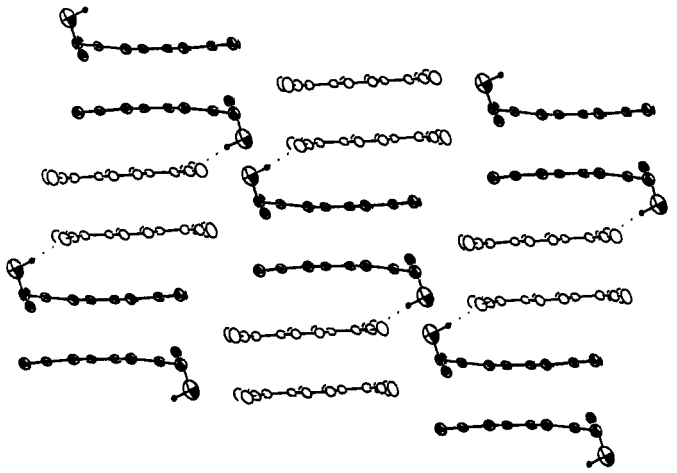

Figure 2. The $\cdots D_2\text{-}A_2\cdots$ mode of stacking along [110] for 8-TCNQ and the hydrogen bond (dotted lines) pattern within the stack.

Table 3. Selected Bond Distances (Å) for 8-TCNQ

atom	atom	dist, Å
	8	
S(1)	C(1)	1.8113(3)
S(2)	C(1)	1.7805(3)
S(3)	C(2)	1.7873(3)
S(4)	C(2)	1.7992(3)
S(1)	C(3)	1.7214(3)
S(2)	C(4)	1.7334(3)
S(3)	C(5)	1.7139(3)
S(4)	C(6)	1.6695(3)
C(1)	C(2)	1.3379(2)
C(3)	C(4)	1.4296(2)
C(5)	C(6)	1.4480(2)
C(7)	O	1.4918(2)
O	H	1.2017(2)
	TCNQ	
C(12)	C(13)	1.4608(2)
C(12)	C(17)	1.5071(3)
C(14)	C(15)	1.4991(3)
C(15)	C(16)	1.4772(2)
C(13)	C(14)	1.2857(2)
C(16)	C(17)	1.2878(2)
C(12)	C(18)	1.3480(2)
C(15)	C(21)	1.3590(2)
C(18)	C(19)	1.5023(3)
C(18)	C(20)	1.4618(2)
C(21)	C(22)	1.4425(2)
C(21)	C(23)	1.5226(3)

stacking axis and the interstack pattern of association shown in Figure 3 is similar to that found in (HMTSeF)-(TCNQ).[27] Within the centrosymmetrical $(8^{\bullet+})_2$ dimer, the molecules adopt a fully eclipsed configuration with an interplanar separation (3.17(1) Å, Figure 4), among the shortest ever observed in such systems. As expected,[28] the molecules are slightly bent with short S···S contacts (3.164(4) and 3.181(4) Å for S(1)···S(4) and S(2)···S(3), respectively). The molecules in $(TCNQ)_2$ are slightly long-axis slipped (0.30(2) Å) and separated by 3.12(1) Å (Figure 4) with bond lengths typical of a fully reduced TCNQ anion radical,[29] suggesting the complex is fully charge-transferred. Accordingly, the material was found to be an electrical insulator and can be properly formulated as

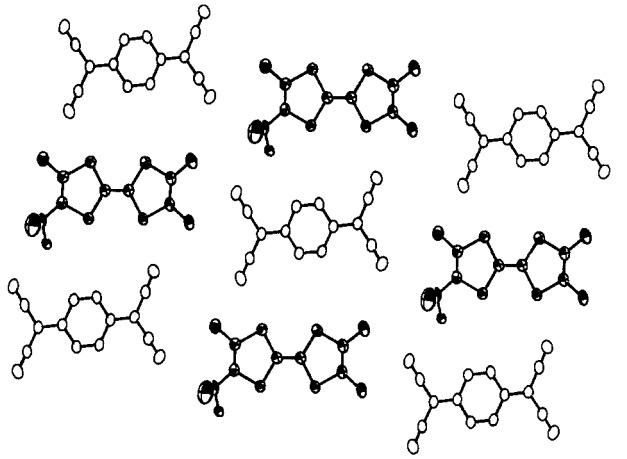

Figure 3. Interstack pattern as viewed in projection down [110] for 8-TCNQ.

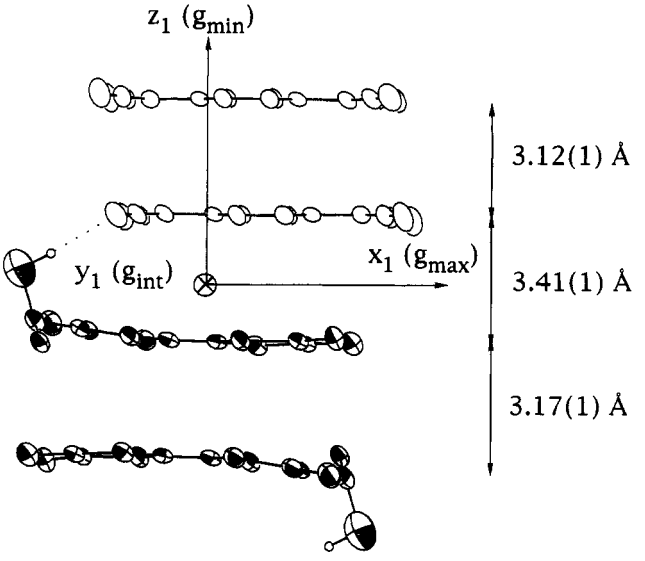

Figure 4. The **g** tensor molecular axis system (x_1, y_1, z_1) as determined, common to both triplet excitations.

$[(\pm)Me_3TTF\text{-}C^*H(Me)OH^{\bullet+}]_2[TCNQ^{\bullet-}]_2$. The interdimer separation along the stack is 3.41(1) Å.

Hydrogen Bonding. The two shortest intermolecular contacts in the structure, O···N(3), 3.24(1) Å and O···N(4), 3.24(1) Å, involve the hydroxyl oxygen atom of the donor molecules and the nitrogen atoms of the two nitrile groups of two different molecules with the potential of establishing interstack and intrastack interactions, respectively. However, only one electron density peak was detected on the difference Fourier map, corresponding to the location of a hydrogen atom at a proper distance from the oxygen atom and pointing toward N(4); hence, the corresponding dotted lines and the subsequent pattern of *intra*stack hydrogen bonded associations shown in Figures 2 and 4. The geometrical characteristics of this O-H···N(4) hydrogen bond are exemplified further in Figure 5. Note that the C-N(4)···H angle amounts to 93°, i.e., well away from the optimum approach (180°) closest to the nitrogen atom. A literature search for hydrogen bonds with nitriles allows one to discriminate between short (strong) hydrogen bonds[30] where the O-H···NC (or N-H···NC) arrangement is linear and longer (weaker) hydrogen bonds[31] (>3.0 Å) where the O···N-C angle varies from 90° to 180°. To rationalize the observed variability in the direction of these (or other) hydrogen bonds, one has to bear in mind that

(26) Grossel, M. C.; Hitchcock, P. B.; Seddon, K. R.; Welton, T.; Weston, S. C., submitted for publication.
(27) Phillips, T. E.; Kistenmacher, T. J.; Bloch, A. N.; Cowan, D. O. *J. Chem. Soc., Chem. Commun.* **1976**, 334.
(28) Batail, P.; Ouahab, L. *Mol. Cryst. Liq. Cryst.* **1985**, *125*, 205.
(29) Flandrois, S.; Chasseau, D. *Acta. Crystallogr. B* **1977**, *33*, 2744.

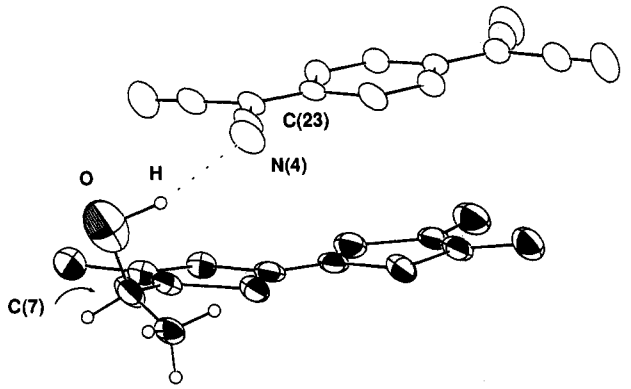

Figure 5. Geometry of the O–H···N hydrogen bond in the crystals of 8–TCNQ: N(4)···H = 2.117(6) Å, O–H···N(4) = 154.4(6)°, C(23)–N(4)···H = 102.0(5)°.

the energy of these primarily electrostatic interactions falls off very slowly with distance.[32] Maps of electrostatic potential (ESP) were determined recently by ab initio SCF calculations for isolated CH_3CN and C_6H_5CN.[33] They are characterized by a minimum located on the symmetry axis of the nitrile group, at 1.32 Å below the nitrogen atom, corresponding to the optimum fixation site distance and direction of approach for an electrophile, in agreement with the geometry of the shortest and strongest hydrogen bonds. The minimum electrostatic potential experienced by a hydrogen atom lying further away from the nitrogen atom, as is the case within the present structure (2.117(6) Å, see Figure 5), becomes more diffuse around the nitrogen atom and appears to be essentially distributed along an envelope around the nucleophilic nitrogen atom, allowing a variety of energetically equivalent approaches with HNC angles much smaller than 180°. Therefore, it is concluded that in 8–TCNQ, a weak hydrogen bond serves to link dimers of π-donor and π-acceptor molecules along the stacks, a rare situation in charge-transfer complexes.[26,34]

ESR Spectra. A representative single-crystal ESR spectrum recorded at room temperature is shown in Figure 6a. It consists of three signals which correspond to typical absorptions of mobile triplet species (Frenkel spin excitons),[24,25b,35] namely, a complex central resonance, the so-called impurity line,[36] two close lateral bands (triplet 2) and two more widely spaced lateral bands (triplet 1). As the temperature decreases, the intensities of the lines for triplet 1 decrease rapidly until they eventually disappear at 255 K. The intensities of the lines of triplet 2 remain constant down to 60 K, then increase until the temperature reaches 10 K when they start decreasing. The ESR spectrum for 8–TCNQ, recorded at 10 K where the

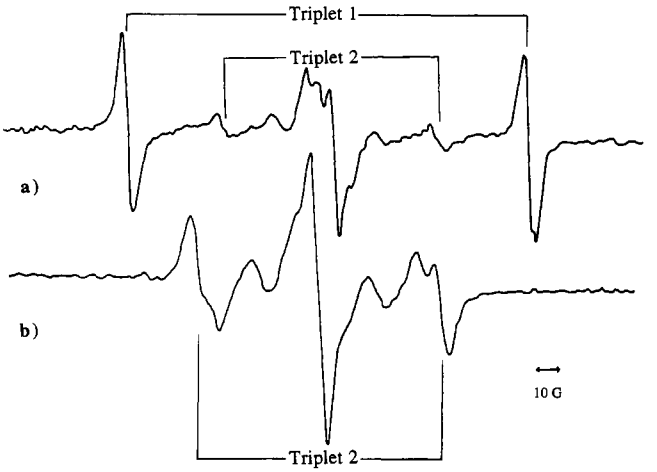

Figure 6. (a) Room-temperature single-crystal ESR spectrum of 8–TCNQ. (b) 10 K single-crystal ESR spectrum of 8–TCNQ, at approximately the same orientation.

Table 4. Principal Axis g Tensor Values for 8–TCNQ and a Series of Relevant Systems

compound	g_{max}	g_{int}	g_{min}	g_{iso}[a]	ref
This Work					
triplet 1	2.0085	2.0048	2.0023	2.0052	
triplet 2	2.0070	2.0048	2.0025	2.0048	
Anion Radical Salts					
vinamidinium-TCNQ[b]	2.0033	2.0027	2.0025	2.0028	30d
$(Ph_3XCH_3)(TCNQ)_2$[c]	2.0040	2.0031	2.0027	2.0033	35b
Cation Radical Salts					
$TMTTF(BF_4)_{0.5}$	2.0106	2.0097	2.0019	2.0074	39
$[(MeS)_4TTF]_2[Mo_6Cl_8(NCS)_6]$	2.0140	2.0075	2.0022	2.0079	35a
$TTF-(Cl)_{0.9}$	2.0127	2.009	2.0026	2.0081	39

[a] $g_{iso} = {}^1/_3(g_{max} + g_{int} + g_{min})$. [b] Vinamidinium = *N,N'*-diphenyl-1,5-diazapentadienium. [c] X = P or As.

triplet 2 resonances intensities are maximum, is given in Figure 6b. It should be noted that similar ESR spectra were consistently obtained for single crystals from several different batches, suggesting that triplet 2 resonances are intrinsic. The absence of hyperfine splitting for the lines of triplet 1 results from a dynamical averaging effect from translation or diffusion of the triplet excitons through the crystal.[37] Note however that the resonance line width (5.5 G) appears somewhat broad for triplet exciton resonances (ca. 1 G) suggesting slow exciton motion.[25b,38] Meanwhile, the quite large ESR line width (8 G) and also perhaps some hyperfine structure of the 10 K spectrum of Figure 6b, observed for triplet 2, may indicate the presence of a localized exciton.

g Tensor. The values of the **g** tensor principal axis (Table 4) have been determined from the angular dependence of the midpoint between the two components of the triplet lines, determined at room temperature for the triplet 1 and at 10 K for triplet 2.[35a] Note (Figure 4) that the **g** tensor principal axis directions are found to match the symmetry axis of both the donor and acceptor molecules, a feature common to the **g** tensors of TTF and TCNQ salts.[35a,39] Clearly, the **g** values for 8–TCNQ are inter-

(30) (a) Higashi, T.; Osaki, K. *Acta. Crystallogr. B* **1978**, *34*, 1393. (b) Truong, K. D.; Bandrauk, A. D.; Ishii, K.; Carlone, C.; Jandl, S. *Mol. Cryst. Liq. Crystallogr.* **1985**, *120*, 105. (c) Kobayashi, H.; Danno, T.; Saito, Y. *Acta. Cryst. B* **1973**, *29*, 2693. (d) Strzelecka, H.; Veber, M.; Zinsou, A.-T.; Bassoul, P.; Petit, P.; Bieber, A.; André, J.-J. *J. Mater. Chem.* **1993**, *3*, 59.

(31) (a) Sundaresan, T.; Wallwork, S. C. *Acta. Crystallogr. B* **1972**, *28*, 3507. (b) Sundaresan, T.; Wallwork, S. C. *Acta. Crystallogr. B* **1972**, *28*, 491.

(32) Vinogradov, S. N.; Linnel, R. H. *Hydrogen Bonding*; Litton Educational Publishing, Inc.: New York, 1971.

(33) Rohmer, M.-M.; Benard, M. *J. Am. Chem. Soc.*, in press.

(34) Inabe, T.; Okaniwa, K.; Okamoto, H.; Mitani, T.; Maruyama, Y.; Tadeka, S. *Mol. Cryst. Liq. Cryst.* **1992**, *216*, 229.

(35) (a) Guirauden, A., Johannsen, I.; Batail, P.; Coulon, C. *Inorg. Chem.* **1993**, *32*, 2446. (b) Chesnut, D. B.; Phillips, W. D. *J. Chem. Phys.* **1961**, *35*, 1002. (c) Chesnut, D. B.; Arthur, P., Jr. *J. Chem. Phys.* **1962**, *36*, 2969. (d) Soos, Z. G. *J. Chem. Phys.* **1967**, *46*, 4284.

(36) Bailey, J. C.; Chesnut, D. B. *J. Chem. Phys.* **1969**, *51*, 5118.

(37) (a) Jones, M. T.; Chesnut, D. B. *J. Chem. Phys.* **1963**, *38*, 1311. (b) Hibma, T. J., Kommandeur, J. *Phys. Rev. B* **1975**, *12*, 2608.

(38) (a) Hove, M. J.; Hoffman, B. M.; Ibers, J. A. *J. Chem. Phys.* **1972**, *56*, 3490. (b) Harms, R. H.; Keller, H. J.; Nöthe, D.; Werner, M.; Gundel, D.; Sixl, H.; Soos, Z. G.; Metzger, R. M. *Mol. Cryst. Liq. Cryst.* **1981**, *65*, 179.

Table 5. Experimental Fine Structure Tensors for 8–TCNQ and the Observed Magnetic Gap

magnetic gap, eV	principal values, G	ZFS params, G	principal axis	principal direction cosines in the molecular axis system (x_1, y_1, z_1)		
				x_1	y_1	z_1
		Triplet 1				
0.326	d_{XX} = 190	D = −403	X	0.99	−0.07	−0.10
	d_{YY} = 79	E = 55	Y	0.1	0.94	0.35
	d_{ZZ} = −269	D/E = −7.3	Z	0.07	−0.35	0.94
		Triplet 2				
0.0001[a]	d_{XX} = 76	D = −168	Z	−0.24	−0.01	0.97
	d_{YY} = 36	E = 20	Y	0.04	−0.99	0.01
	d_{ZZ} = −112	D/E = −8.4	Z	0.97	0.03	0.24

[a] This value is not very accurate because of the lack of experimental points at low temperature.

mediate (Table 4) between those obtained for either TTF-based or TCNQ-based salts.

Singlet–Triplet Energy Separation and Zero-Field Splitting (ZFS) Parameters. The activation energies of the two triplet excitons have been obtained from the observed temperature dependences of the intensities of the resonance signals ($I = A/T[\exp(E_a/k_BT) + 3]^{-1}$).[35] The two symmetrical lateral bands for triplets 1 and 2 occur at two different fields separated by δH (Figure 6). The variation of δH upon rotations of the crystal around three orthogonal axes were determined at room temperature for triplet 1 and at 10 K for triplet 2. Thus the zero-field splitting (ZFS) tensors are obtained and diagonalized to give the ZFS parameters, D and E, listed in Table 5 ($D = {}^3/_2 d_{ZZ}$; $E = {}^1/_2(d_{XX} - d_{YY})$),[35] where Z is the direction of maximum zero-field splitting. Note that all three principal axes of the fine structure tensor lie near the principal axis directions (x_1, y_1, z_1)[35a] of the **g** tensor (Table 5) as symbolized in Figure 4. However, while the maximum ZFS for triplet 1, Z, lies close to z_1, it is observed to be near x_1 for triplet 2 along the longer molecular axis, i.e., the horizontal interchain axis direction in Figure 3. Both the orientation of the fine structure tensor and the magnitude of the ZFS parameters (D and E) are indicative of the origin and location of the triplet exciton.[25b,35,40] Thus, given the observed orientations reported above, it is concluded that triplet 1 is due to *intra*chain Frenkel excitations while triplet 2 is due to *inter*chain Frenkel excitations (in the direction of the long axis of the molecule, Figure 3). The latter is consistent with smaller D and E values for triplet 2, also because such smaller values reflect the larger spin density separation between the molecules in the transverse interchain direction. It should be noted[41] that the low intensity of triplet 2 compared to the "impurity" signal in either Figures 6a or 6b suggests that exciton 2 consists of adjacent misfit $TTF^{\bullet+}$ and $TCNQ^{\bullet-}$ in adjacent stacks. In fact, exciton 2 could perhaps be identified as some sort of structural defect or low-concentration impurity species, as indicated by its lack of motion. Indeed, no motion is expected for such defects.

Calculated Intradimer Transfer Integral. The intermolecular transfer integrals have been obtained by extended Hückel calculations using single-ζ type orbitals. Typically, single-ζ intradimer transfer integral t values are 0.185 eV for the moderately coupled dimers in $[(MeS)_4TTF^{\bullet+}]_2[Mo_6Cl_8(NCS)_6^{2-}]$ and 0.425 eV for the strongly coupled ESR-silent dimers in TTF-I_3.[35a] It is found that in 8–TCNQ, within each dimer the molecules are strongly interacting with transfer integral t values amounting to 0.58 eV for $(8^{\bullet+})_2$ and 0.265 eV for $(TCNQ^{\bullet-})_2$. Note that on the basis of the large t value for $(8^{\bullet+})_2$, no ESR triplet activity is expected for this dimer in the compound.

Conclusion

In this paper we have shown that the use of a racemic mixture of the chiral π-donor molecule, (±)Me_3-TTFC*HMeOH, has indeed resulted in the construction of the charge-transfer salt $[(\pm)Me_3TTF\text{-}C^*H(Me)OH^{\bullet+}][TCNQ^{\bullet-}]$ whose molecular solid-state architecture is based on *centrosymmetrical* dimers. Thus, two different types of dimers have been engaged within an unprecedented ···DDAA··· mixed stack pattern. A single *intra*stack O–H···N hydrogen bond was found to effectively anchor the DD and AA dimers along the stack. The compound exhibits two different kinds of singlet–triplet excitations, characterized by single-crystal ESR experiments. The major singlet–triplet excitation (0.326 eV) was found to be essentially localized on the $(TCNQ^{\bullet-})_2$ dimers, while another considerably weaker singlet-triplet excitation (0.0001 eV) is more likely the result of an interchain coupling.

Acknowledgment. We thank Marie-Liesse Doublet and Enric Canadell for transfer integral calculations and Marc Bénard, Marie-Madeleine Romer, and Martin Grossel for helpful discussions and communication of their results prior to publication.

Supplementary Material Available: Tables of atomic coordinates of all atoms, bond lengths, bond angles and anisotropic thermal parameters for all non-hydrogen atoms (5 pages); listing of calculated and observed structure factors (12 pages). Ordering information is given on any current masthead page.

(39) Walsh, W. M., Jr.; Rupp, L. W., Jr.; Wudl, F.; Kaplan, M. L.; Schafer, D. E.; Thomas, G. A.; Gemmer, R. *Solid State Commun.* **1980**, *33*, 413.
(40) Silverstein, A. J.; Soos, Z. G. *Chem. Phys. Lett.* **1976**, *39*, 525.
(41) We thank one reviewer for insightful comments on that matter.